High-level ab initio study of disulfur monoxide: Ground state potential energy surface and band origins for six isotopic species

Oleg Egorov, Michael M. Rey, Roman Kochanov, Andrei Nikitin, Vladimir Tyuterev

▶ **To cite this version:**

Oleg Egorov, Michael M. Rey, Roman Kochanov, Andrei Nikitin, Vladimir Tyuterev. High-level ab initio study of disulfur monoxide: Ground state potential energy surface and band origins for six isotopic species. Chemical Physics Letters, 2023, 811, pp.140216. 10.1016/j.cplett.2022.140216 . hal-04283830

HAL Id: hal-04283830
https://hal.science/hal-04283830

Submitted on 14 Nov 2023

HAL is a multi-disciplinary open access archive for the deposit and dissemination of scientific research documents, whether they are published or not. The documents may come from teaching and research institutions in France or abroad, or from public or private research centers.

L'archive ouverte pluridisciplinaire **HAL**, est destinée au dépôt et à la diffusion de documents scientifiques de niveau recherche, publiés ou non, émanant des établissements d'enseignement et de recherche français ou étrangers, des laboratoires publics ou privés.

High-level *ab initio* study of disulfur monoxide: ground state potential energy surface and band origins for six isotopic species

Oleg Egorov[1,2*], Michaël Rey[3], Roman V. Kochanov[1,2], Andrei V. Nikitin[1,2], Vladimir Tyuterev[2,3]

[1]Laboratory of Theoretical Spectroscopy, V.E. Zuev Institute of Atmospheric Optics SB RAS 1, Akademician Zuev Sq., Tomsk, 634055 Russia

[2]Tomsk State University 36, Lenin Ave., Tomsk, 634050 Russia

[3]Groupe de Spectrométrie Moléculaire et Atmosphérique UMR CNRS 7331, UFR Sciences BP 1039, 51687 Reims Cedex 2, France

Corresponding Author

*(O.E.) E-mail: oleg.egorov@iao.ru

Abstract

In this work, a series of potential energy surfaces (PESs) of S_2O was constructed in order to get the most accurate *ab initio* band origins of this massive molecule. The convergence of the coupled cluster energies with respect to both basis set size [aug-cc-pCVXZ, X=T, Q, 5, and 6] and the order of the excitation [CC(*n*), *n* = 2, 3, and 4] was analyzed. For the first time, the band origins of $^{32}S_2{}^{16(18)}O$ were variationally calculated with the error of 0.5 cm^{-1} using the *ab initio* PES. The vibrational energies of the most abundant six isotopologues of S_2O were predicted.

Keywords: disulfur monoxide, ground state, *ab initio*, potential energy surface, band origins.

I. Introduction

A good knowledge of spectral properties of sulfur containing species is important for various ecological applications including the detection of volcanoes gas emissions, which are a natural source of sulfur oxides in the atmospheres [1]. Among small sulfur containing molecules, disulfur monoxide (S_2O) was relatively less investigated in terms of full-dimensional *ab initio* potential energy surfaces (PESs) compared to, for example, SO_2 and SO_3 [2–4, and reference therein].

In the early spectroscopic studies by Schenk [5], S_2O was associated with some unknown species belonging to a lower oxide of sulfur ("sulfur monoxide") which is produced by a high voltage electric discharge in a mixture of sulfur vapor and SO_2. The infrared and ultraviolet spectra examined after by Jones [6] suggested that the molecular geometry could correspond to the C_{2v} point group. For this reason, the observed spectra cannot occur due to the diatomic SO, but rather due to $S_2O_2(C_{2v})$, which was proposed in [6, 7]. The unambiguous and dominant presence of S_2O in samples (prepared in the same way as in [5, 6]) was established by Meschi and Myers [8] by mass spectrographic and molecular weight analyses.

According to the microwave spectra studied by Meschi and Myers [9], Cook et al. [10], and Tiemann et al. [11], S_2O has a bent S–S–O structure with a bond angle of 118°; two components of its permanent dipole moment are both nonzero at the equilibrium configuration [9]. The accurate substitution r_S structure was determined by Lindenmayer [12] using the rotational transitions of four isotopic species ($^{32}S_2{}^{16}O$, $^{34}S^{32}S^{16}O$, $^{32}S^{34}S^{16}O$, and $^{32}S_2{}^{18}O$). Information on the rotational transitions were then extended by Thorwith et al. [13] who observed the vibrational satellites from 14 excited vibrational states including the first detection of the ^{33}SSO and $S^{33}SO$ species.

The Doppler-limited diode laser spectra recorded by Lindenmayer with coauthors [14, 15] allowed to resolve several hundred rovibrational transitions belonging to the stretching ν_1 and ν_3 bands of both $^{32}S_2{}^{16}O$ and $^{32}S_2{}^{18}O$. The high-resolution study in the region of the low frequency bending mode were carried out recently at the SOLEIL synchrotron facility by Martin-Drumel et al. [16]. Accurate sets of molecular parameters for the (000), (010) and (020) states were determined by combining both the far-infrared and millimeter-wave measurements. The high-frequency part of the recorded synchrotron spectra included the ν_3 and $\nu_3+\nu_2-\nu_2$ bands which were later analyzed in [17].

Vibronic transitions into the first excited electronic state of S_2O ($\tilde{C}^1A' \leftarrow \tilde{X}^1A'$) were the subject to a variety of experimental and theoretical studies [18–21, and references therein]. Particularly, pre-dissociative features of the $\tilde{C}^1A'$ state were examined by Zhang et al. [21] from the observed vibronic progression associated with the S-S stretching mode. The monotonically decreasing collision-free lifetimes for bands with $\upsilon(\text{S-S}) \geq 3$ indicated on the existing the pre-dissociation process that can be due to the intersection with the repulsive $\tilde{D}^1A'$ state at energies of

about υ = 6. The vicinity of the $\tilde{C}^1A'$ and $\tilde{D}^1A'$ states at larger S-S bond length agrees with the theoretical predictions [22, 23]. According to Muller et al. [24], the vibrational structure of the $\tilde{X}^1A'$ state has a local-mode character and it can be satisfactory reproduced without nondiagonal resonance terms up to ~13000 cm^{-1} in contrast to that of the $\tilde{C}^1A'$ state. Along with the asymmetric bent S_2O, two isomers of the C_{2v} symmetry (cyclic and open-SOS) are possible. The spectrum of the cyclic-SOS was assigned by Lo et al. [25, 26] while open-SOS was not observed. These two isomers can have a close frequency of the asymmetric S-O stretch whereas their intensities differ about one order of the magnitude as it was calculated by Denis [27].

Without a doubt, the construction of the variationally computed line list of S_2O will help to interpret its high-resolution spectra including the line intensities of cold and hot bands. To this end, we have systematically applied high-level *ab initio* methods to calculate the potential energies of S_2O in its ground electronic state in order to construct an accurate PES. Next section gives the details of the analytical model of the PES as well as *ab initio* and variational approaches applied in this work. Obtained results are discussed in Section III, followed by the conclusion in Section IV.

II. Method

The analytical model of the S_2O (C_s) PES was expressed as a Taylor series expansion by the powers of the following 3 coordinates

$$\begin{cases} S_1 = 1 - \exp\left[-b_{SS}\cdot\left(r(SS) - r_e(SS)\right)\right] \\ S_2 = \cos(\alpha) - \cos(\alpha_e) \\ S_3 = 1 - \exp\left[-b_{SO}\cdot\left(r(SO) - r_e(SO)\right)\right] \end{cases}, \quad (1)$$

where b_{SS} = 2.3 $Å^{-1}$ and b_{SO} = 2.8 $Å^{-1}$. The grid of the nuclear configurations of S_2O was constructed by sampling its two bond lengths [r(SS) and r(SO)] and one bond angle [$\alpha \equiv \angle$SSO]. The *total* grid included 1362 points covering the 0–7000 cm^{-1} energy range. Although the correct dissociation limit is out of the aim of this work, the D_e(S–SO) value in our PES well correlates with the experimental estimation (~30000 cm^{-1} [21]). The *ab initio* energies were fitted with the RMS error not greater than 0.4 cm^{-1} using 60 expansion terms.

The single- and double-excitation coupled cluster method with a perturbative treatment of triple excitations [CCSD(T)] implemented in the MOLPRO package [28] was employed as a "basic" approach in this work. The main advantages of CCSD(T) are well-known: it provides smooth and size-consistent *ab initio* energies. Moreover, the contribution from the high-order excited determinants can be included into the PES by the consecutive scaling to the triples (CCSDT), quadruples (CCSDTQ), pentuples (CCSDTQP), and other high-levels of the excitation available in the MRCC package [29]. Since the cost of the calculations rapidly increases with the excitation level,

the CCSDT and CCSDT(Q) methods were applied with cc-pVTZ basis set (hereafter, VTZ) while for CCSDTQ, the cc-pVDZ basis set (hereafter, VDZ) was used. Note that the convergence of the contributions of the high-order excitations is actually fast with respect to the basis set size as it was demonstrated for different molecules, for example, [30].

The energies of the CCSD(T) method were kept close to the complete basis set limit (CBS) by employing the Dunning's augmented correlation-consistent orbital basis sets with the core-valence electron correlation [aug-cc-pCVXZ, hereafter, ACVXZ, X=T, Q, 5, and 6]. Total *ab initio* energies (Hartree-Fock+correlation) were then extrapolated with respect to the basis set size using the following functional:

$$E_X = E_{CBS} + A \cdot \exp\left(-\left(X-1\right)\right) + B \cdot \exp\left(-\left(X-1\right)^2\right). \quad (2)$$

In addition, we tested the explicitly-correlated F12x{x=a, b} versions of CCSD(T) in a combination with the cc-pCVQZ-F12 (hereafter, CVQZ-F12) basis set that provides the accuracy comparable with the CCSD(T)/ACV6Z level with less computation costs [31].

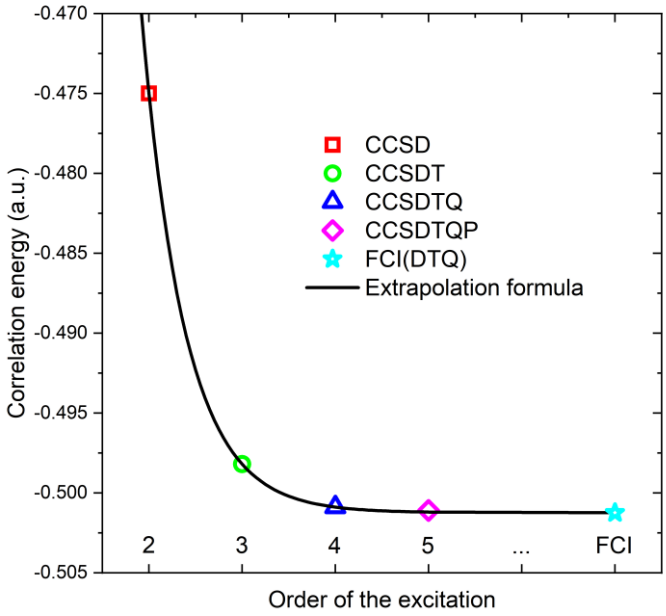

Fig.1. Typical dependence of the correlation energy on the order of the excitation. Solid line is the three-point extrapolation by Eq. (3) without the energy of the CCSDTQP level

As it will be seen in the next Section, the contribution of the high-order excitations changes the *ab initio* band origins of S_2O very significantly. Although it is possible to achieve the agreement between the theory and experiment within 1 cm^{-1} by combining the ACV5Z basis set with the excitations up to the CCSDTQ level (see Table II), it is evident that the correlation energy of the quadruple level is far from the full configuration interaction (FCI) limit. Since one point at the

CCSDTQP/VDZ level already takes about 1 month, we extrapolated the coupled cluster energies to the FCI limit as follows

$$E_n = E_{FCI} + A \cdot \exp(-C \cdot n), \quad (3)$$

where E_n and E_{FCI} are correlation energies (without Hartree-Fock contribution); n corresponds to the level of the excitation: n = 2 (CCSD), n = 3 (CCSDT), and n = 4 (CCSDTQ). Note that the correlation energies of the same basis set size (VDZ) were considered in Eq (3) and these energies were reproduced by Eq. (3) with the error less than 10^{-8} a.u. An example of the extrapolation is demonstrated in Fig. 1 for the first point in our grid (r(SS)=1.89070475 Å, r(SO)=1.45935399 Å, and α=118º) for which the correlation energy of the CCSDTQP/VDZ level was additionally calculated. The reader can see the exponential type behavior that is true for all other points given in Supplementary Materials (file "fci(dtq)_info.dat").

Along with the high-order electronic excitations, the contributions due to the scalar relativistic effects (relativistic) and diagonal Born-Oppenheimer correction (DBOC) were included into the PESs. The relativistic correction was calculated using the Douglas-Kroll-Hess (DKH) scalar relativistic Hamiltonian available in MOLPRO. The DKH Hamiltonian of the eighth order was combined with the ACVTZ-DK basis set. The energy contributions from higher order transformations were found to be less than 10^{-4} cm^{-1}. DBOC was calculated at the HF-CCSD/VTZ level in the CFOUR package [32] using the nuclear masses of the main $^{32}S_2{}^{16}O$ isotopologue.

The *total* grid composed of 1362 nuclear configurations was applied for calculating the *ab initio* energies using the CCSD(T)/ACVTZ and CCSD(T)/ACVTZ-DK methods as well as for the explicitly correlated [CCSD(T)-F12x{x=a, b}/CVQZ-F12] version, and when computing the DBOC. The time demanding but high-quality methods were employed for the limited number points of the grid in order to get the smooth energy differences which were then fitted and extrapolated for the nuclear configurations of the *total* grid. Particularly, the CCSD(T)/[ACVQZ–ACVTZ] and CCSD(T)/[ACV5Z–ACVTZ] energy differences computed for 400 nuclear configurations were fitted with the RMS deviation of 0.05 cm^{-1} using the PES expansion including the 4th order terms. For the largest currently feasible ACV6Z basis set, the CCSD(T) energies were calculated for 110 points while the contributions from the high-order electronic correlations, namely [CCSDT-CCSD(T)]/VTZ, [CCSDT(Q)-CCSDT]/VTZ, and [CCSDTQ-CCSDT(Q)]/VDZ, were included from 200 points. It is worth mentioning that a similar strategy for constructing *ab initio* PESs was also applied for other molecules (see, for example, CH_4 [33], H_2CO [34], NH_3 [35], C_2H_2 [36], and CH_3 [36]). All the *ab initio* energies calculated in this work are available in Supplementary Materials.

The nuclear motion calculations were carried out from our home-made variational computer code TENSOR [38–41] applied with success for computing accurate spectroscopic line lists of semirigid and nonrigid molecules [42–46, and references therein]. To achieve a convergence better

than 10^{-4} cm^{-1} for the vibrational levels up to 5000 cm^{-1}, 5456 basis functions were used for the symmetry block A'. As an additional test of the convergence, we applied the well-known DVR3D computer code [47]. For all the vibrational levels considered in this work, the difference between these two methods was found to be less than 10^{-4} cm^{-1} which confirmed the choice of our vibrational basis set. Note also that contrary to DVR3D, the TENSOR computer code provides eigenvalues with a full quantum assignment. For all variational calculations presented below, the atomic masses were employed in the kinetic energy operator to approximately include the non-adiabatic effects (see [48] for more details).

III. Results and discussion

In this article we follow a conventional vibrational assignment for triatomic molecules: υ_2 is the bending mode while υ_1 and υ_3 are the S–O and S–S stretching ones, respectively. All vibrational levels have the same symmetry A'. Consequently, the symmetry label will be omitted hereafter.

Table I. *Ab initio* equilibrium geometry of S_2O at the CCSD(T) level of theory

Level	r_e(SS)	r_e(SO)	α_e(Deg.)	E_0(a.u.)
CCSD(T)/ACVTZ	1.897083	1.466116	117.79500	–871.3246099228
CCSD(T)/ACVQZ	1.884423	1.456646	117.96889	–871.4949855247
CCSD(T)/ACV5Z	1.881262	1.454058	117.95978	–871.5621707188
CCSD(T)/ACV6Z	1.879938	1.453343	117.96394	–871.5849793841
CCSD(T)-F12b/CVQZ-F12	1.880035	1.453169	117.96188	–871.5855095621
CCSD(T)-F12a/CVQZ-F12	1.879956	1.453238	117.96264	–871.5984315610
CCSD(T)/CBS(TQ56Z)	1.879298	1.452747	117.96005	–871.5997821471
CCSD(T)/CBS(TQ5Z)	1.879438	1.452568	117.95355	–871.6013307853

Notes: the presented geometries correspond to the bottom of the fitted PESs. Bond lengths are in Ångström; bond angle is in degrees.
E_0 is the *ab initio* energy at the equilibrium geometry.

The impact of the size of the basis set on the equilibrium geometry of S_2O at the CCSD(T) level can be seen from **Table I**. The explicitly-correlated F12x{x=a, b} methods give rather accurate results: the corresponding values lie between those provided by the largest ACV6Z basis set and those obtained by the extrapolation to the CBS limit. Below we will consider two variants of the extrapolation: when the CCSD(T)/ACV6Z energies are included or not in order to analyze how much the accuracy of the final vibrational levels can be improved. At this stage, one can see that the bottom of the CCSD(T)/CBS(TQ5Z) PES is a little bit lower than that of the CCSD(T)/CBS(TQ56Z) one.

Table II. *Ab initio* band origins (in cm^{-1}) of $^{32}S_2{}^{16}O$ at the CCSDTQ (first line) and extrapolated FCI (second line) levels of the theory compared to the high-resolution measurements

Band	Exp.	Exp. – Calc.							
		ACVTZ	ACVQZ	ACV5Z	ACV6Z	F12a	F12b	CBS(TQ5Z)	CBS(TQ56Z)
ν_2	380.310[a]	**9.340**	**2.435**	**0.366**	–0.213	–0.205	–0.340	–0.827	–0.675
		9.975	3.022	0.940	**0.355**	**0.364**	**0.228**	**–0.261**	**–0.109**
ν_3	679.136[b]	**19.647**	**3.150**	**–0.169**	–2.045	–2.679	–2.715	–2.054	–2.567
		22.147	5.426	2.051	**0.155**	**–0.483**	**–0.517**	**0.134**	**–0.378**
$2\nu_2$	760.386[a]	**18.721**	**4.901**	**0.775**	–0.400	–0.386	–0.657	–1.607	–1.307
		19.994	6.078	1.927	**0.741**	**0.757**	**0.485**	**–0.470**	**–0.171**
$\nu_2+\nu_3$	1056.936[b]	**28.978**	**5.558**	**0.179**	–2.280	–2.912	–3.087	–2.898	–3.258
		32.134	8.441	2.993	**0.509**	**–0.127**	**–0.301**	**–0.123**	**–0.483**
ν_1	1166.454[c]	**24.470**	**7.419**	**0.670**	–0.902	–1.401	–1.802	–3.281	–2.511
		27.475	10.208	3.405	**1.814**	**1.313**	**0.910**	**–0.576**	**0.197**
Total RMS		**21.271**	**5.016**	**0.499**	1.442	1.888	2.034	2.309	2.266
		23.568	7.085	2.423	**0.922**	**0.732**	**0.543**	**0.362**	**0.302**

Notes: all our PESs included the following corrections: relativistic, DBOC, and high-order electronic correlations – up to the CCSDTQ level (first line) and up to the extrapolated FCI limit (second line). The details can be found in section II. The best result (in terms of rms) for each basis set is highlighted by **bold font**.
[a]Martin-Drumel et al. [16];
[b]Thorwirth et al. [17];
[c]Lindenmayer et al. [15].

Table III. Impact of the corrections on the equilibrium geometry of $^{32}S_2{}^{16}O$

Level	r_e(SS)	r_e(SO)	α_e(Deg.)
CCSD(T)/CBS(TQ56Z)	1.879298	1.452747	117.96005
+Relativistic(ACVTZ-DK)	1.879657	1.453036	117.96619
+DBOC(CCSD/VTZ)	1.879659	1.453043	117.96410
+CCSDT/VTZ	1.879798	1.452479	117.89744
+CCSDT(Q)/VTZ	1.884849	1.456234	117.86653
+CCSDTQ/VDZ	1.883727	1.455242	117.86443
+FCI(DTQ)/VDZ	1.884348	1.455670	117.85870
Empirical[a]	1.88424(11)	1.45621(13)	117.876(4)

Notes: presented geometries correspond to the bottom of the fitted PESs. Bond lengths are in Ångström; bond angle is in degrees.
[a]Obtained by Lindenmayer et al. [15] without accurate infrared data on the ν_2 band.

In the case of S_2O the accuracy of the predicted band origins depends mainly on two factors: the basis set size and the order of the electronic excitations. Although both factors lead to the increase of the absolute value of the correlation energy, their contribution to the calculated band origins has opposite signs. According to **Table II**, "Exp.–Calc." values gradually decrease when going from the "ACVTZ" to "ACV5Z" columns and then they change the sign at "ACV6Z" (see first lines in the mentioned columns). In other words, the completeness of the basis set size has a positive contribution to the predicted band origins. The completeness of the electronic correlations, on the contrary, results in diminishing of some energy values that becomes evident when comparing the results given in the first and second lines for each basis set size in **Table II**.

Particularly, we found that the PES constructed by combining the ACV5Z basis set size with the electronic correlations up to the CCSDTQ level provides rather accurate *ab initio* band origins of S_2O (with the rms deviation of 0.50 cm^{-1}). However, for the next ACV6Z basis set the CCSDTQ level is not enough to compensate the growth in band origins. The same is true for the explicitly-correlated F12x{x=a, b} methods as well as for two extrapolations with respect to the basis set size. To achieve a better agreement, the contributions from the higher-order electronic correlations have to be included in the cases of the bigger basis set sizes. Note that for molecules such as NH_3 [35] or CH_3 [37], the CCSDT(Q) level was enough for reaching an agreement within 1 cm^{-1} in band origins, even under the CBS limit since the contributions from the CCSDTQ and CCSDTQP levels were relatively small. Since the complete inclusion of the CCSDTQP level was not computationally feasible so far for S_2O, we made the extrapolation to the FCI level as it was previously discussed in Section II. As a result, the band origins calculated from the CBS(TQ56Z) PES became the most accurate ones (rms deviation of 0.30 cm^{-1}). Another CBS(TQ5Z) PES provides comparable results with rms deviation of 0.36 cm^{-1} and turns out to be the best choice if the computationally cost ACV6Z basis set is not considered.

Table IV. Impact of the corrections on the band origins of $^{32}S_2{}^{16}O$

Band			+Rel.	+DBOC	+CCSDT	+CCSDT(Q)	+CCSDTQ	+FCI(DTQ)	Total
V_1	V_2	V_3							
0	1	0	–1.070	0.043	0.266	–4.971	1.289	–0.566	–5.009
0	0	1	–2.044	0.018	0.071	–15.810	4.344	–2.189	–15.609
0	2	0	–2.144	0.086	0.500	–9.903	2.530	–1.137	–10.068
0	1	1	–3.109	0.061	0.314	–20.824	5.627	–2.775	–20.707
0	3	0	–3.224	0.130	0.702	–14.798	3.726	–1.712	–15.176
1	0	0	–3.478	0.019	3.501	–24.307	8.292	–2.708	–18.680
0	0	2	–4.068	0.037	0.222	–32.103	8.897	–4.471	–31.486
0	2	1	–4.180	0.104	0.525	–25.799	6.861	–3.366	–25.854
0	4	0	–4.309	0.174	0.876	–19.661	4.879	–2.293	–20.333
1	1	0	–4.549	0.061	3.711	–29.248	9.511	–3.283	–23.796
0	1	2	–5.130	0.079	0.439	–37.153	10.168	–5.077	–36.674
0	3	1	–5.256	0.148	0.705	–30.736	8.050	–3.961	–31.050
1	0	1	–5.510	0.037	3.477	–40.070	12.520	–4.930	–34.476
0	5	0	–5.400	0.220	1.024	–24.499	5.996	–2.879	–25.539
1	2	0	–5.624	0.104	3.887	–34.140	10.677	–3.862	–28.957
0	0	3	–6.073	0.054	0.453	–48.846	13.646	–6.841	–47.607
0	2	2	–6.197	0.122	0.624	–42.165	11.391	–5.688	–41.912
0	4	1	–6.337	0.193	0.857	–35.640	9.196	–4.562	–36.293
1	1	1	–6.577	0.080	3.673	–45.068	13.745	–5.526	–39.673
0	6	0	–6.497	0.266	1.147	–29.322	7.083	–3.472	–30.795
1	3	0	–6.704	0.148	4.031	–38.985	11.792	–4.445	–34.162
2	0	0	–6.923	0.037	7.321	–49.928	17.354	–5.545	–37.685
0	1	3	–7.132	0.097	0.640	–53.928	14.902	–7.466	–52.886
0	3	2	–7.269	0.166	0.779	–47.139	12.569	–6.303	–47.196

1	0	2	–7.522	0.056	3.532	–56.358	16.966	–7.254	–50.581
0	5	1	–7.425	0.238	0.983	–40.513	10.302	–5.167	–41.582
1	2	1	–7.648	0.123	3.836	–50.021	14.920	–6.125	–44.916
0	7	0	–7.600	0.313	1.250	–34.145	8.150	–4.074	–36.106
1	4	0	–7.789	0.193	4.145	–43.791	12.864	–5.031	–39.409
0	0	4	–7.996	0.079	7.465	–59.664	18.578	–9.290	–50.827
2	1	0	–8.061	0.072	0.759	–61.147	18.479	–6.129	–56.027
0	2	3	–8.196	0.141	0.797	–58.971	16.111	–8.096	–58.214
0	4	2	–8.347	0.211	0.907	–52.079	13.704	–6.923	–52.527
1	1	2	–8.585	0.098	3.706	–61.400	18.188	–7.869	–55.863
0	6	1	–8.518	0.285	1.083	–45.363	11.373	–5.779	–46.918
1	3	1	–8.724	0.167	3.968	–54.930	16.046	–6.729	–50.203
2	0	1	–8.945	0.055	7.208	–65.638	21.466	–7.801	–53.654
0	8	0	–8.710	0.361	1.337	–38.992	9.214	–4.685	–41.476
1	5	0	–8.879	0.239	4.233	–48.579	13.908	–5.624	–44.702
0	1	4	–9.072	0.123	7.568	–68.785	19.815	–9.934	–60.285
2	2	0	–9.116	0.115	0.916	–61.902	19.506	–6.711	–57.194
0	3	3	–9.265	0.185	0.924	–63.977	17.274	–8.730	–63.589
1	0	3	–9.515	0.074	3.662	–73.162	21.631	–9.677	–66.987
0	5	2	–9.431	0.257	1.008	–56.987	14.799	–7.548	–57.902
1	2	2	–9.652	0.141	3.848	–66.400	19.360	–8.489	–61.191
0	7	1	–9.617	0.332	1.162	–50.195	12.413	–6.397	–52.301
0	0	5	–9.805	0.211	4.070	–64.835	22.163	–10.296	–58.492
1	4	1	–10.032	0.090	1.137	–78.484	18.638	–8.850	–77.500
2	1	1	–10.012	0.097	7.356	–70.619	22.633	–8.407	–58.951
0	9	0	–9.827	0.408	1.412	–43.901	10.303	–5.310	–46.916

Notes: given values are the differences in the band origins (in cm^{-1}) when the corresponding correction is taken into account. For example, the "DBOC" column means the difference in the band origins calculated at the [CCSD(T)/CBS(TQ56Z)+Relativistic+DBOC] and [CCSD(T)/CBS(TQ56Z)+Relativistic] levels of the theory.
First 50 levels are presented. A total list up to 5000 cm^{-1} is given in Supplementary Materials.

As it was expected, the corrections due to the high-order electronic correlations had the biggest contributions to the potential energies of S_2O while the effect of DBOC was the smallest one (**Tables III** and **IV**). According to **Table III**, a good agreement was obtained for the equilibrium geometry after adding all the corrections. Moreover, we have estimated the pure *ab initio* rotational constants of the ground vibrational state by applying a novel approach [49] for deriving effective Hamiltonians directly from *ab initio* PESs without using perturbation theory. It led to the following values (in MHz): A_0 = 41913.2435, B_0 = 5060.6425, and C_0 = 4508.0907 which agree within 2.2, –1.55, and –0.93 MHz respectively with the recent empirical data from [16].

Among the three types of vibrational modes, the inclusion of the high-order electronic correlations was significant for all the vibrational bands involving the stretches (υ_1 and υ_3). Although this is a "usual" situation for the most of the molecules it should be mentioned that the corresponding contributions were extremely large even for the fundamentals, namely ≈15 cm^{-1} and ≈13 cm^{-1} for ν_1 and ν_3, respectively. This means that CCSD(T) gives rather approximate results for molecules with a large number of electrons. Another interesting feature associated with the coupled cluster approaches

can be seen from the differences between the accurate and perturbative levels: both CCSD(T) and CCSDT(Q) overestimated the contribution of the correlation energy into the band origins of S_2O. A similar result was already obtained for NH_3 [35], for which the CCSDTQ-CCSDT(Q) difference was also of positive sign.

The shifts due to the relativistic effects cannot be neglected as well. The minimal contributions were about of 1, 2, and 3 cm^{-1} for the ν_2, ν_3, and ν_1 bands, respectively, and then they proportionally increased for overtones and combination bands. Finally, DBOC took the third place in terms of contributions: ≈0.02 cm^{-1} for ν_3 and ν_1, and ≈0.04 cm^{-1} for ν_2.

Table V. *Ab initio* band origins (in cm^{-1}) for the $^{32}S_2{}^{18}O$ isotopologue compared to the available high-resolution measurements by Lindenmayer et al. [15]

Band	Exp.	Calc.	Exp. – Calc.
ν_3	677.322	677.702	–0.380
ν_1	1124.757	1124.561	0.196

Note: the CBS(TQ56Z) PES was applied for variational calculations.

Table VI. Band origins of the most abundant six isotopic species of S_2O predicted from our final *ab initio* PES

Band			$^{32}S_2{}^{16}O$ (0.900117)	$^{32}S^{34}S^{16}O$ (0.040273)	$^{34}S^{32}S^{16}O$ (0.040273)	$^{32}S^{33}S^{16}O$ (0.007107)	$^{33}S^{32}S^{16}O$ (0.007107)	$^{32}S_2{}^{18}O$ (0.001850)
V_1	V_2	V_3						
0	1	0	380.419	377.765	377.6157	379.0675	378.986	369.237
0	0	1	679.514	669.866	670.1701	674.5556	674.705	677.702
0	2	0	760.557	755.247	754.9528	757.8537	757.693	738.223
0	1	1	1057.419	1045.186	1045.356	1051.145	1051.221	1044.387
0	3	0	1140.418	1132.452	1132.017	1136.363	1136.126	1106.959
1	0	0	1166.257	1154.351	1166.051	1160.126	1166.152	1124.561
0	0	2	1353.206	1334.008	1334.782	1343.34	1343.722	1349.586
0	2	1	1435.049	1420.230	1420.268	1427.458	1427.464	1410.833
0	4	0	1520.003	1509.378	1508.808	1514.594	1514.284	1475.439
1	1	0	1543.952	1529.443	1540.923	1536.496	1542.402	1491.351
0	1	2	1728.643	1706.928	1707.574	1717.496	1717.809	1713.794
0	3	1	1812.410	1795.003	1794.912	1803.502	1803.438	1777.04
1	0	1	1844.476	1823.090	1834.738	1833.474	1839.469	1801.069
0	5	0	1899.307	1886.019	1885.326	1892.542	1892.165	1843.649
1	2	0	1921.386	1904.274	1915.53	1912.605	1918.390	1857.924
0	0	3	2021.159	1992.505	1993.941	2006.433	2007.144	2015.703
0	2	2	2103.811	2079.577	2080.097	2091.381	2091.627	2077.77
0	4	1	2189.503	2169.506	2169.29	2179.276	2179.145	2143.009
1	1	1	2219.549	2195.634	2207.097	2207.259	2213.156	2165.123
0	6	0	2278.318	2262.364	2261.564	2270.195	2269.761	2211.568
1	3	0	2298.565	2278.851	2289.88	2288.46	2294.121	2224.28
2	0	0	2316.368	2292.843	2315.949	2304.253	2316.151	2234.283
0	1	3	2394.166	2363.061	2364.372	2378.192	2378.837	2377.489
0	3	2	2478.715	2451.960	2452.357	2465.002	2465.182	2441.516
1	0	2	2516.526	2485.780	2497.456	2500.714	2506.721	2471.501

0	5	1	2566.326	2543.737	2543.402	2554.78	2554.585	2508.731
1	2	1	2594.364	2567.918	2579.197	2580.787	2586.585	2528.963
0	7	0	2657.020	2638.390	2637.512	2647.536	2647.060	2579.159
1	4	0	2675.490	2653.174	2663.976	2664.06	2669.598	2590.405
0	0	4	2683.477	2645.454	2647.778	2663.935	2665.090	2676.115
2	1	0	2691.393	2665.321	2688.106	2677.982	2689.706	2598.769
0	2	3	2766.908	2733.350	2734.538	2749.686	2750.265	2739.049
0	4	2	2853.358	2824.080	2824.357	2838.361	2838.477	2805.034
1	1	2	2889.054	2855.849	2867.359	2871.991	2877.911	2832.964
0	6	1	2942.872	2917.689	2917.242	2930.005	2929.750	2874.196
1	3	1	2968.931	2939.952	2951.044	2954.064	2959.763	2892.595
2	0	1	2993.534	2960.684	2983.441	2976.629	2988.346	2909.768
0	8	0	3035.390	3014.068	3013.155	3024.536	3024.044	2946.367
1	5	0	3052.153	3027.231	3037.816	3039.397	3044.817	2956.256
0	1	4	3054.087	3013.679	3015.88	3033.332	3034.420	3035.522
2	2	0	3066.207	3037.604	3060.026	3051.507	3063.033	2963.183
0	3	3	3139.393	3103.379	3104.445	3120.921	3121.435	3100.385
1	0	3	3182.414	3142.423	3154.216	3161.851	3167.917	3135.869
0	5	2	3227.739	3195.937	3196.095	3211.457	3211.510	3168.319
1	2	2	3261.329	3225.662	3237.006	3243.013	3248.845	3194.217
0	7	1	3319.130	3291.348	3290.804	3304.94	3304.633	3239.384
0	0	5	3340.292	3292.982	3296.461	3315.978	3317.707	3330.901
1	4	1	3343.251	3311.740	3322.643	3327.096	3332.693	3271.173
2	1	1	3365.765	3330.445	3352.962	3347.603	3359.194	3313.107
0	9	0	3413.392	3389.351	3388.476	3401.157	3400.689	3321.725

Notes:
ZPE($^{32}S_2{}^{16}O$) = 1122.814 cm^{-1}
ZPE($^{32}S^{34}S^{16}O$) = 1110.478 cm^{-1}
ZPE($^{34}S^{32}S^{16}O$) = 1116.608 cm^{-1}
ZPE($^{32}S^{33}S^{16}O$) = 1116.474 cm^{-1}
ZPE($^{33}S^{32}S^{16}O$) = 1119.625 cm^{-1}
ZPE($^{32}S_2{}^{18}O$) = 1094.885 cm^{-1}
Abundances are given in brackets. The applied *ab initio* CBS(TQ56Z) PES included the contribution of the DBOC of the main isotopologue ($^{32}S_2{}^{16}O$) in all cases. The shift due to DBOC is small compared to other corrections (0.14 cm^{-1} in average in **Table IV**). The dependence of DBOC on isotopic masses was estimated as ~0.01 cm^{-1}.
The first 50 levels are presented. The complete list up to 5000 cm^{-1} is given in Supplementary Materials.

Note that the abundance of the ^{34}S isotope is about 4 % which is rather big when comparing, for example, with ^{13}C (1 %) or ^{18}O (0.2 %). The microwave spectra of $^{34}S^{32}S^{16}O$ and $^{32}S^{34}S^{16}O$ were observed in the early work by Tiemann et al. [11]. The rotational transitions of $^{32}S_2{}^{18}O$ were also recorded later by Lindenmayer [12] both in its ground and first vibrational (bending) state. Thorwith et al. [13] detected the rotational spectra of $^{33}S^{32}S^{16}O$ and $^{32}S^{33}S^{16}O$ for the first time. To our knowledge, the infrared spectra of the minor species were less studied. For example, Lindenmayer et al. [15] presented the empirical molecular parameters of the ν_3 and ν_1 bands of $^{32}S_2{}^{18}O$. The corresponding band origins agree within 0.4 cm^{-1} with the calculated from the CBS(TQ56Z) *ab initio* PES (**Table V**).

Since the six above mentioned isotopologues give a considerable contribution to the absorption spectra of S_2O in natural abundance, we have provided for the very first time in this work the whole set of accurate vibrational levels up to 5000 cm^{-1} for all these species. According to **Table VI**, when the central atom ^{32}S is substituted by the heavier ones (^{34}S and ^{33}S) the frequency of the bending mode changes less than those of the two stretches. As expected, the substitution of the outer sulfur (oxygen) impacts mainly on the bending and the S–S (S–O) stretching modes. Note that the predicted origins of the ν_2 and ν_3 bands of $^{34}S^{32}S^{16}O$ and $^{32}S^{34}S^{16}O$ differ by 0.3 cm^{-1} while those of $^{33}S^{32}S^{16}O$ and $^{32}S^{33}S^{16}O$ differ by only 0.2 cm^{-1}. The abundancies of these two isotopologues being the same, their spectra can be more easily resolved by analyzing those bands where the υ_1 mode is involved.

IV. Conclusions

In this work, 16 *ab initio* potential energy surfaces (PESs) of S_2O were constructed and validated. For the first time, the agreement within 1 cm^{-1} was achieved for all band origins which were experimentally studied by high-resolution. As the best compromise (less demanding in terms of computational resources and accurate in terms of band origins), it was shown that an accurate *ab initio* PES can be obtained by making the calculations with the CCSD(T)/aug-cc-pCV5Z method and including the corrections from the quadruple level [CCSDTQ] of the electronic excitations. In the case of the complete basis set (CBS) limit, the CCSDTQ level becomes insufficient but the correlation energy can be further included by the extrapolation to the full configuration interaction (FCI) limit. It allowed to calculate the band origins of $^{32}S_2{}^{16}O$ and $^{32}S_2{}^{18}O$ with the error of 0.5 cm^{-1} by applying the CBS(TQ56Z) PES. Note that the CBS(TQ5Z) PES provided results within 0.1 cm^{-1} in terms of rms deviation. Similarly to the CBS limit, the accuracy of the extrapolated FCI limit can be increased if the correlation energies of higher orders of the excitation (particularly, CCSDTQP) will be included into the extrapolation functional. The achieved accuracy can be considered as one of the proofs of the validity of the advanced *ab initio* methods for molecules with a relatively large number of electrons.

The band origins of the most abundant six isotopic species of S_2O predicted from the validated *ab initio* PES can be applied as a good starting point for further high-resolution studies of these unstable species.

Supplementary Material

Supplementary Materials include the C++ code for the analytical models of the constructed the most accurate *ab initio* PESs; the *ab initio* points for the nuclear configurations considered in this work; the band origins of the six isotopic species predicted up to 5000 cm^{-1}.

Acknowledgements

This work was supported by a Grant from the RF Ministry of Education and Science for the project "SACHA": (N 075-15-2021-1412, contract identifier RF2251.62321X0012) in a framework of bilateral French-Russian "Kolmogorov" (PHC) cooperation program (2021-2251-ΠΠ408) for Science and Technology.

References

[1] M.Yu. Zolotov, B.Jr. Fegley, Volcanic Origin of Disulfur Monoxide (S_2O) on Io, Icarus 133(2) (1998) 293–297, https://doi.org/10.1006/icar.1998.5930

[2] D.S. Underwood, S.N. Yurchenko, J. Tennyson, A.F. Al-Refaie, S. Clausen, A. Fateev, ExoMol molecular line lists – XVII. The rotation–vibration spectrum of hot SO_3, MNRAS 462 (2016) 4300–4313, https://doi.org/10.1093/mnras/stw1828

[3] X. Huang, D.W. Schwenke, T.J. Lee, Isotopologue consistency of semi-empirically computed infrared line lists and further improvement for rare isotopologues: CO_2 and SO_2 case studies, J. Quant. Spectrosc. Radiat. Transfer 230 (2019) 222–246, https://doi.org/10.1016/j.jqsrt.2019.03.002

[4] J. Li, Y. Ding, Z. Li, Z. Peng, Simultaneous measurements of SO_2 and SO_3 in the heterogeneous conversions of SO2 using QCL absorption spectroscopy, Applied Physics B 128 (2022) 61, https://doi.org/10.1007/s00340-022-07776-0

[5] P.W. Schenk, Über das Schwefelmonoxyd, Zeits. f. anorg. allgem. Chemie 211 (1933) 150–160.

[6] V.A. Jones, Infra-Red and Ultraviolet Spectra of Sulphur Monoxide, J. Chem. Phys. 18 (1950) 1263, https://doi.org/10.1063/1.1747922

[7] E. Kondrat'eva, V. Kondrat'ev, Zh. Fiz. Khim. 14 (1940) 1528.

[8] D.J. Meschi, R.J. Myers, Disulfur Monoxide. I. Its Identification as the Major Constituent in Schenk's "Sulfur Monoxide", J. Am. Chem. Soc. 78(24) (1956) 6220–6223, https://doi.org/10.1021/ja01605a002

[9] D.J. Meschi, R.J. Myers, The microwave spectrum, structure, and dipole moment of disulfur monoxide, J. Mol. Spectrosc. 3(1-6) (1959) 405–416, https://doi.org/10.1016/0022-2852(59)90036-0

[10] R.L. Cook, G. Winnewisser, D.C. Lindsey, The centrifugal distortion constants of disulfur monoxide, J. Mol. Spectrosc. 46(2) 1973 276–284, https://doi.org/10.1016/0022-2852(73)90042-8

[11] E. Tiemann, J. Hoeft, F.J. Lovas, D.R. Johnson, Spectroscopic studies of the SO_2 discharge system. I. The microwave spectrum and structure of S_2O, J. Chem. Phys. 60 (1974) 5000–5004, http://dx.doi.org/10.1063/1.1681014

[12] J. Lindenmayer, The rs structure of disulfur monoxide: The microwave spectrum of $S_2{}^{18}O$, J. Mol. Spectrosc. 116(2) (1986) 315–319, https://doi.org/10.1016/0022-2852(86)90129-3

[13] S. Thorwirth, P. Theulé, C.A. Gottlieb, H.S.P. Müller, M.C. McCarthy, P. Thaddeus, Rotational spectroscopy of S_2O: Vibrational satellites, ^{33}S isotopomers, and the sub-millimeter-wave spectrum, J. Mol. Structure. 795(1–3) (2006) 219–229, https://doi.org/10.1016/j.molstruc.2006.02.055

[14] J. Lindenmayer, H. Jones, The diode-laser spectrum of the ν1 band of disulfur monoxide, J. Mol. Spectrosc. 112(1) (1985) 71–78, https://doi.org/10.1016/0022-2852(85)90192-4

[15] J. Lindenmayer, H.D. Rudolph, H. Jones, The equilibrium structure of disulfur monoxide: Diode laser spectroscopy of ν_1 and ν_3 of $S_2{}^{18}O$ and ν_3 of $S_2{}^{16}O$, J. Mol. Spectrosc. 119(1) (1986) 56–67, https://doi.org/10.1016/0022-2852(86)90201-8

[16] M.A. Martin-Drumel, C.P. Endres, O. Zingsheim, T. Salomon, J. van Wijngaarden, O. Pirali, S. Gruet, F. Lewen, S. Schlemmer, M.C. McCarthy, S. Thorwirth, The SOLEIL view on sulfur rich oxides: The S_2O bending mode at 380 cm^{-1} and its analysis using an Automated Spectral Assignment Procedure (ASAP), J. Mol. Spectrosc. 315 (2015) 72–79, https://doi.org/10.1016/j.jms.2015.02.014

[17] S. Thorwirth, M.A. Martin-Drumel, C.P. Endres, T. Salomon, O. Zingsheim, J. van Wijngaarden, O. Pirali, S. Gruet, F. Lewen, S. Schlemmer, M.C. McCarthy, An ASAP treatment of vibrationally excited S_2O: The ν_3 mode and the $\nu_3 + \nu_2 - \nu_2$ hot band, J. Mol. Spectrosc. (319) 2016 47–49, https://doi.org/10.1016/j.jms.2015.12.009

[18] G. Lakshminarayana, Ultraviolet band systems of S_2O, J. Mol. Spectrosc. 55(1–3) (1975) 141–150, https://doi.org/10.1016/0022-2852(75)90259-3

[19] K-E.J. Hallin, A.J. Merer, D.J. Milton, Rotational analysis of bands of the 3400 Å system of disulphur monoxide (S_2O), Can. J. Phys. 55(21) (1977) 1858–1867, https://doi.org/10.1139/p77-226

[20] C.L. Chiu, P.C. Sung, L.D. Chen, Excitation and fluorescence spectra of disulfur monoxide, J. Mol. Spectrosc. 94(2) (1982) 343–350, https://doi.org/10.1016/0022-2852(82)90010-8

[21] Q. Zhang, P. Dupré, B. Grzybowski, P.H. Vaccaro, Laser-induced fluorescence studies of jet-cooled S_2O: Axis-switching and predissociation effects, J. Chem. Phys. 103 (1995) 67–79, https://doi.org/10.1063/1.469623

[22] T.J. Dudley, M.R. Hoffmann, Theoretical study of the ground and first excited singlet state potential energy surfaces of disulphur monoxide (S_2O), Mol. Physics. 101(9) (2003) 1303–1310, https://doi.org/10.1080/0026897031000075660
[23] H. Han, B. Suo, Z. Jiang, Y. Wang, Z. Wen, The potential energy curves of low-lying electronic states of S_2O // J. Chem. Phys. 128 (2008) 184312, https://doi.org/10.1063/1.2917236
[24] T. Müller, P.H. Vaccaro, F. Pérez-Bernal, F. Iachello, The vibronically-resolved emission spectrum of disulfur monoxide An algebraic calculation and quantitative interpretation of Franck–Condon transition intensities, J. Chem. Phys 111(11) (1999) 5038–5055, https://doi.org/10.1063/1.479786
[25] W-J. Lo, Y-J. Wu, Y-P. Lee, Isomers of Infrared absorption spectra of cyclic in solid Ar, J. Chem. Phys. 117 (2002) 6655, https://doi.org/10.1063/1.1506155
[26] W-J. Lo, Y-J. Wu, Y-P. Lee, Ultraviolet Absorption Spectrum of Cyclic S_2O in Solid Ar, J. Phys. Chem. A 107(36), (2003) 6944–6947, https://doi.org/10.1021/jp034563j
[27] P.A. Denis, Theoretical characterisation of the SSO, cyclic SOS and SOS isomers, Mol. Physics 108(2) (2010) 171–179, http://dx.doi.org/10.1080/00268970903580166
[28] H.-J. Werner, P.J. Knowles, F.R. Manby, J.A. Black, K. Doll, A. Heßelmann, D. Kats, A. Köhn, T. Korona, D.A. Kreplin, Q. Ma, T.F. Miller, A. Mitrushchenkov, K.A. Peterson, I. Polyak, G. Rauhut, M. Sibaev, The Molpro quantum chemistry package, J. Chem. Phys. 152 (2020) 144107, https://doi.org/10.1063/5.0005081
[29] M. Kállay, P.R. Nagy, D. Mester, Z. Rolik, G. Samu, J. Csontos, J. Csóka, P.B. Szabó, L. Gyevi-Nagy, B. Hégely, I. Ladjánszki, L. Szegedy, B. Ladóczki, K. Petrov, M. Farkas, P.D. Mezei, A. Ganyecz, The MRCC program system: Accurate quantum chemistry from water to proteins, J. Chem. Phys. 152 (2020) 074107, https://doi.org/10.1063/1.5142048
[30] A.D. Boese, M. Oren, O. Atasoylu, M.L. Jan Martin, M. Kállay, J. Gauss, W3 theory: Robust computational thermochemistry in the kJ/mol accuracy range, J. Chem. Phys. 120 (2004) 4129–4141, https://doi.org/10.1063/1.1638736
[31] J.G. Hill, S. Mazumder, K.A. Peterson, Correlation consistent basis sets for molecular core-valence effects with explicitly correlated wave functions: The atoms B–Ne and Al–Ar, J. Chem. Phys. 132 (2010) 054108, https://doi.org/10.1063/1.3308483
[32] D.A. Matthews, L. Cheng, M.E. Harding, F. Lipparini, S. Stopkowicz, T.-C. Jagau, P.G. Szalay, J. Gauss, J.F. Stanton, Coupled-Cluster Techniques for Computational Chemistry: the CFOUR Program Package, J. Chem. Phys. 152 (2020) 214108, https://doi.org/10.1063/5.0004837
[33] A.V. Nikitin, M. Rey, Vl.G. Tyuterev, First fully ab initio potential energy surface of methane with a spectroscopic accuracy, J. Chem. Phys. 145 (2016) 114309, http://dx.doi.org/10.1063/1.4961973
[34] A.V. Nikitin, A.E. Protasevich, A.A. Rodina, M. Rey, A. Tajti, V.G. Tyuterev, Vibrational levels of formaldehyde: Calculations from new high precision potential energy surfaces and comparison with experimental band origins, J. Quant. Spectrosc. Radiat. Transfer 260 (2021) 107478, https://doi.org/10.1016/j.jqsrt.2020.107478
[35] O. Egorov, M. Rey, A. Nikitin, V. Dominika, New Ab Initio Potential Energy Surfaces for NH_3 Constructed from Explicitly Correlated Coupled-Cluster Methods, J. Phys. Chem. A 125(49) (2021) 10568–10579, https://doi.org/10.1021/acs.jpca.1c08717
[36] A.V. Nikitin, A.E. Protasevich, A.A. Rodina, M. Rey, A. Tajti, V.G. Tyuterev, Ro-vibrational levels and their (e-f) splitting of acetylene molecule calculated from new potential energy surfaces, J. Quant. Spectrosc. Radiat. Transfer 292 (2022) 108349, https://doi.org/10.1016/j.jqsrt.2022.108349
[37] O. Egorov, M. Rey, A.V. Nikitin, D. Viglaska, New Theoretical Infrared Line List for the Methyl Radical with Accurate Vibrational Band Origins from High-Level Ab Initio, J. Phys. Chem. A 126 (2022) 6429−6442, https://doi.org/10.1021/acs.jpca.2c04822
[38] M. Rey, A.V. Nikitin, Vl.G. Tyuterev, Ab initio ro-vibrational Hamiltonian in irreducible tensor formalism: a method for computing energy levels from potential energy surfaces for symmetric-top molecules, Mol. Phys. 108 (2010) 2121–2135, https://doi.org/10.1080/00268976.2010.506892
[39] M. Rey, A.V. Nikitin, Vl.G. Tyuterev, Complete nuclear motion Hamiltonian in the irreducible normal mode tensor operator formalism for the methane molecule, J. Chem. Phys. 136 (2012) 244106, https://doi.org/10.1063/1.4730030
[40] M. Rey, Group-theoretical formulation of an Eckart-frame kinetic energy operator in curvilinear coordinates for polyatomic molecules, J. Chem. Phys. 151 (2019) 024101, https://doi.org/10.1063/1.5109482
[41] D. Viglaska, M. Rey, A.V. Nikitin, V.G. Tyuterev, Derivation of ρ-dependent coordinate transformations for nonrigid molecules in the Hougen–Bunker–Johns formalism, J. Chem. Phys. 153 (2020) 084102, https://doi.org/10.1063/5.0016365
[42] M. Rey, A.V. Nikitin, V.G. Tyuterev, Accurate Theoretical Methane Line Lists in the Infrared up to 3000 K and Quasi-continuum Absorption/Emission Modeling for Astrophysical Applications, The Astrophysical Journal 847 (2017) 105, https://doi.org/10.3847/1538-4357/aa8909
[43] M. Rey, I.S. Chizhmakova, A.V. Nikitin, V.G. Tyuterev, Understanding global infrared opacity and hot bands of greenhouse molecules with low vibrational modes from first-principles calculations: the case of CF_4, Phys. Chem. Chem. Phys. 20 (2018) 21008, https://doi.org/10.1039/C8CP03252A
[44] O. Egorov, A. Nikitin, M. Rey, A. Rodina, S. Tashkun, V. Tyuterev, Global modeling of NF_3 line positions and intensities from far to mid-infrared up to 2200 cm^{-1}, J. Quant. Spectrosc. Radiat. Transfer 239 (2019) 106668, https://doi.org/10.1016/j.jqsrt.2019.106668

[45] D. Viglaska-Aflalo, M. Rey, A. Nikitin, T. Delahay, A global view of isotopic effects on ro-vibrational spectra of six-atomic molecules: a case study of eleven ethylene species, Phys. Chem. Chem. Phys. 22 (2020) 3204–3216, https://doi.org/10.1039/C9CP06383H
[46] M. Rey, I.S. Chizhmakova, A.V. Nikitin, V.G. Tyuterev, Towards a complete elucidation of the ro-vibrational band structure in the SF_6 infrared spectrum from full quantum-mechanical calculations, Phys. Chem. Chem. Phys. 23 (2021) 12115–12126, https://doi.org/10.1039/D0CP05727D
[47] J. Tennyson, M.A. Kostin, P. Barletta, G.J. Harris, O.L. Polyansky, J. Ramanlal, N.F. Zobov, DVR3D: a program suite for the calculation of rotation–vibration spectra of triatomic molecules. Comp. Phys. Comm. 163(2) (2004) 85–116, https://doi.org/10.1016/j.cpc.2003.10.003
[48] W. Kutzelnigg Which masses are vibrating or rotating in a molecule? Mol. Phys. 105 (2007) 2627–2647, http://dx.doi.org/10.1080/00268970701604671
[49] M. Rey Novel methodology for systematically constructing global effective models from ab initio-based surfaces: A new insight into high-resolution molecular spectra analysis, J. Chem. Phys. 156 (2022) 224103, https://doi.org/10.1063/5.0089097

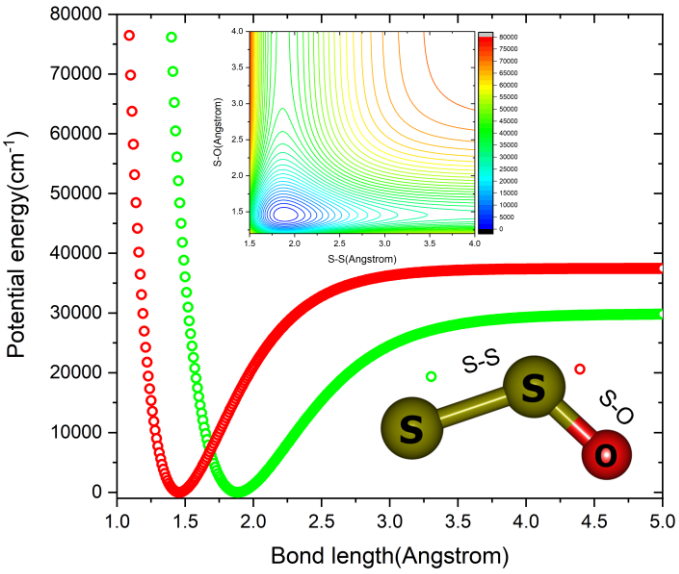

Graphical Abstract